iScience

CellPress
OPEN ACCESS

Article

Characterizing fitness and immune escape of SARS-CoV-2 EG.5 sublineage using elderly serum and nasal organoid

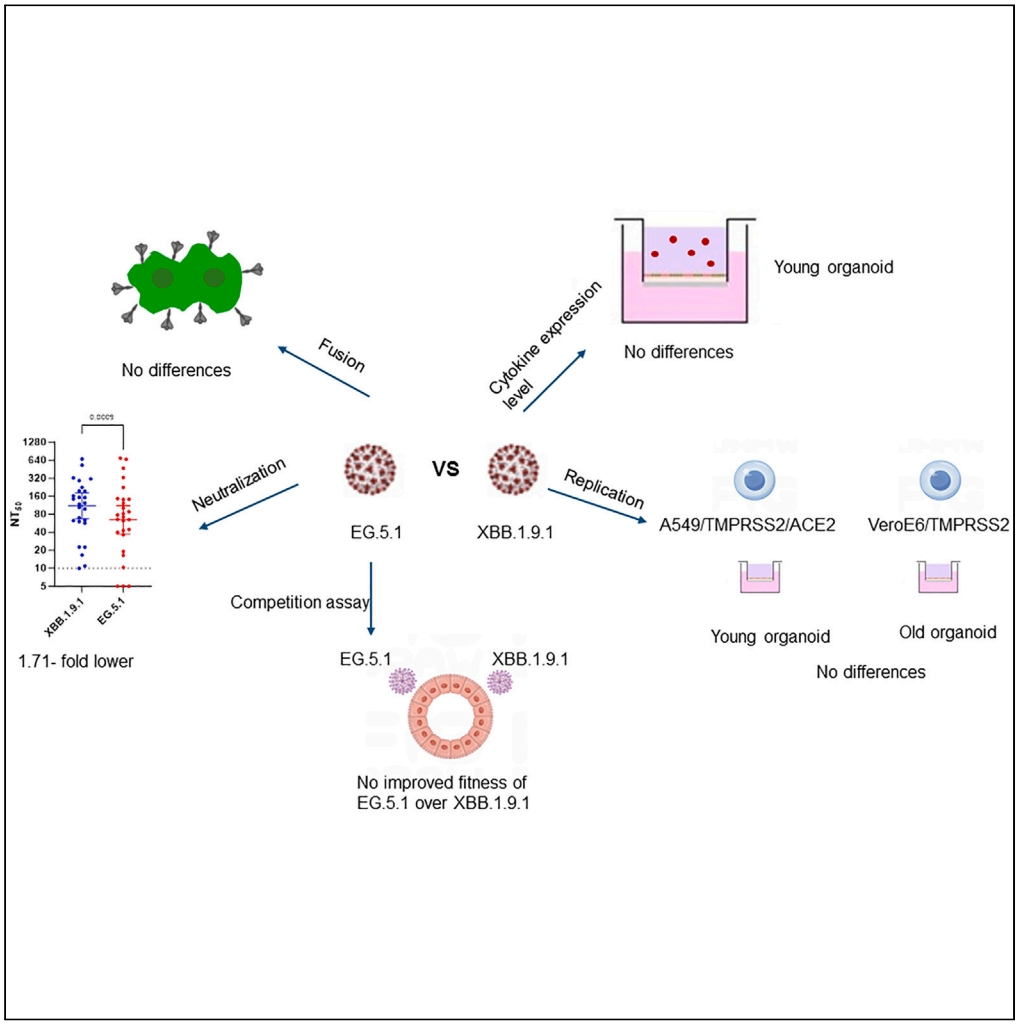

Xiaojuan Zhang, Stephanie Joy-Ann Lam, Jonathan Daniel Ip, ..., Kwok-Yung Yuen, Jie Zhou, Kelvin Kai-Wang To

kelvinto@hku.hk

Highlights

EG.5.1 is more immune evasive than XBB.1.9.1

EG.5.1 exhibited similar viral fitness to XBB.1.9.1

EG.5.1 elicited similar cytokine/chemokine response to XBB.1.9.1

Viral replication was slower in nasal organoid from an older donor

Zhang et al., iScience 27, 109706
May 17, 2024
https://doi.org/10.1016/j.isci.2024.109706

iScience

CellPress
OPEN ACCESS

Article

Characterizing fitness and immune escape of SARS-CoV-2 EG.5 sublineage using elderly serum and nasal organoid

Xiaojuan Zhang,[1,6] Stephanie Joy-Ann Lam,[1,2,6] Jonathan Daniel Ip,[1,6] Carol Ho-Yan Fong,[1,2,6] Allen Wing-Ho Chu,[1,2] Wan-Mui Chan,[1] Yoyo Suet-Yiu Lai,[1,2] Hoi-Wah Tsoi,[1] Brian Pui-Chun Chan,[1] Lin-Lei Chen,[1,2] Xinjie Meng,[1] Shuofeng Yuan,[1,2] Hanjun Zhao,[1,2] Vincent Chi-Chung Cheng,[1,3] Jacqueline Kwan Yuk Yuen,[4] Kwok-Yung Yuen,[1,2,3,5] Jie Zhou,[1,2] and Kelvin Kai-Wang To[1,2,3,5,7,*]

SUMMARY

SARS-CoV-2 Omicron variant has evolved into sublineages. Here, we compared the neutralization susceptibility and viral fitness of EG.5.1 and XBB.1.9.1. Serum neutralization antibody titer against EG.5.1 was 1.71-fold lower than that for XBB.1.9.1. However, there was no significant difference in virus replication between EG.5.1 and XBB.1.9.1 in human nasal organoids and TMPRSS2/ACE2 over-expressing A549 cells. No significant difference was observed in competitive fitness and cytokine/chemokine response between EG.5.1 and XBB.1.9.1. Both EG.5.1 and XBB.1.9.1 replicated more robustly in the nasal organoid from a younger adult than that from an older adult. Our findings suggest that enhanced immune escape contributes to the dominance of EG.5.1 over earlier sublineages. The combination of population serum susceptibility testing and viral fitness evaluation with nasal organoids may hold promise in risk assessment of upcoming variants. Utilization of serum specimens and nasal organoid derived from older adults provides a targeted risk assessment for this vulnerable population.

INTRODUCTION

Since the emergence of SARS-CoV-2 in 2019, worldwide effort in viral genomic surveillance has revealed sequential appearance of SARS-CoV-2 variants.[1] The World Health Organization has highlighted epidemiologically important variants as variants of concern (VOC), variants of interest (VOI), and variants under monitoring (VUM). These variants may have better growth rate, better viral fitness, higher virulence and/or increased immune escape. For example, the Omicron variant, first detected with genomic surveillance in Botswana and South Africa in November 2021 and now become the dominant variant,[2,3] exhibited marked immune escape,[4,5] better fitness than Delta in the presence of serum from vaccinees,[6] and shorter doubling time.[7,8] In 2022, several Omicron sublineages have gradually emerged and become the dominant strain, including the BA.1, BA.2, BA.5 and BQ.1.[1,9]

XBB, a recombinant of BA.2.10.1 and BA.2.75, emerged in August 2022. Patients with prior vaccination or infection had a markedly lower neutralizing titers against XBB than previous Omicron sublineages.[10] XBB outcompeted other sublineages and has become the dominant sublineage in 2023. Within the XBB epidemic, XBB.1.5 (January 2023), XBB.1.9 (March-April 2023), XBB.1.16 (April 2023) and XBB.2.3 (May 2023) have become prevalent and was designated as variants of interest (VOI) or variants under monitoring (VUM) by the World Health Organization.[11] EG.5, a descendant of XBB.1.9 (XBB.1.9.2 with F456L mutation), was designated as a VOI on 9th August 2023 because the rapid increase in prevalence and immune escape.[12,13] According to the World Health Organization, over 90% of SARS-CoV-2 strains belong to the Omicron variant XBB sublineage, and about half belong to the EG.5 or its descendants in October 2023.[14]

SARS-CoV-2 primarily replicates in the nasal epithelium in humans. Hence, the nasal organoid may be a more physiologically relevant model for studying viral fitness than immortal cell lines or animal models. We have previously established well-differentiated human nasal organoids consisting of ciliated cells, goblet cells and club cells.[15] We have used the human nasal organoids to demonstrate the more robust

[1]State Key Laboratory for Emerging Infectious Diseases, Carol Yu Centre for Infection, Department of Microbiology, School of Clinical Medicine, Li Ka Shing Faculty of Medicine, The University of Hong Kong, Pokfulam, Hong Kong Special Administrative Region, China
[2]Centre for Virology, Vaccinology and Therapeutics, Hong Kong Science and Technology Park, Hong Kong Special Administrative Region, China
[3]Department of Microbiology, Queen Mary Hospital, Pokfulam, Hong Kong Special Administrative Region, China
[4]Division of Geriatric Medicine, Department of Medicine, School of Clinical Medicine, Li Ka Shing Faculty of Medicine, The University of Hong Kong, Pokfulam, Hong Kong Special Administrative Region, China
[5]Department of Infectious Disease and Microbiology, The University of Hong Kong-Shenzhen Hospital, Shenzhen, China
[6]These authors contributed equally
[7]Lead contact
*Correspondence: kelvinto@hku.hk
https://doi.org/10.1016/j.isci.2024.109706

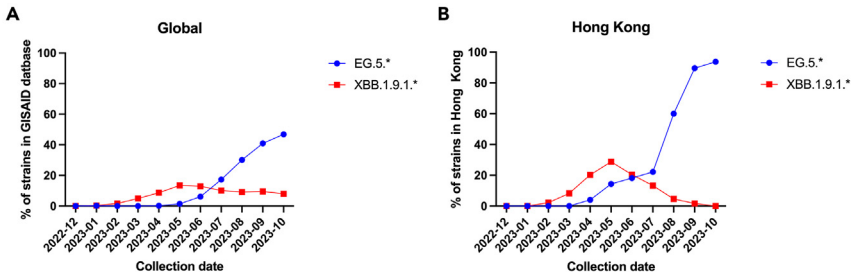

Figure 1. Temporal trend of EG.5 and XBB.1.9.1

(A) Global; (B) Hong Kong. The global data of SARS-CoV-2 were obtained from GISAID on 6th November 2023.

infection of Omicron BA.5 than the BA.1 or ancestral strain.[16] The aim of the current study is to use the human nasal organoids to compare the fitness of EG.5.1 (a descendant of XBB.1.9.2) and the closely related XBB.1.9.1 which EG.5 have replaced.

RESULTS

Emergence of XBB.1.9.1.* and EG.5.* globally

The proportion of XBB.1.9.1 or its sublineages (XBB.1.9.1.*) first exceeded 1% globally and in Hong Kong in February 2023, and peaked in May 2023 (13.48% globally; 28.83% in Hong Kong) (Figure 1). The proportion of EG.5 or it sublineage (EG.5.*) exceeded 1% in May 2023, and overtook XBB.1.9.1 and its sublineages since July 2023. In October 2023, while the proportion of EG.5.* reached 93.8% in Hong Kong, the proportion of EG.5.* reached only 46.9% globally. In view of the dominance of EG.5.*, we proceeded to determine whether the possible reason for dominance. EG.5, when compared with XBB.1.9.1, carries the additional mutations ORF1a A690V (nsp2 A510V) and A3143V (nsp4 A390V) and the spike F456L. EG.5.1, when compared with EG.5, carries an additional spike mutation Q52H.

Comparison of susceptibility to serum neutralization between EG.5.1 and XBB.1.9.1

Since EG.5.1 replaced other XBB sublineages, we hypothesized that EG.5.1 is less susceptible to serum neutralization in our population. We compared the serum neutralization titers between EG.5.1 and XBB.1.9.1 using a live virus neutralization assay. We included serum specimens from 33 patients which were collected in August 2023 (Table S1). All 33 patients received at least 2 doses of vaccines; 17 received BNT162b2 only, 12 received CoronaVac only, and 4 received both BNT162b2 and CoronaVac. 16 had prior infection, of whom 12 had infection in 2022 and 4 had infection in 2023.

Of the 33 patients, 6 did not have detectable levels of neutralizing antibody (nAb) against either XBB.1.9.1 or EG.5.1. Excluding these 6 patients, the nAb titer against EG.5.1 was lower than that against XBB.1.9.1 for 85.2% (23/27) of patients. The geometric mean 50% neutralizing antibody titer (NT_{50} GMT) was 1.71-fold lower for EG.5.1 (GMT: 64.52; 95% CI: 37.4–111.2) than XBB.1.9.1 (GMT: 110.4; 95% CI: 67.2–181.3) ($p = 0.0009$; Wilcoxon matched pairs signed rank test) (Figure 2).

Viral replication kinetics and competition assays

In our previous study, we found that BA.5 replicated better than BA.1 in nasal organoid.[16] Here, we compared the viral replication between EG.5.1 and BA.5.2 in the nasal organoid. The viral load was significantly higher for EG.5.1 than BA.5.2 at 24 and 48 hpi (Figure S1).

Next, we compared the replication kinetics between EG.5.1 and XBB.1.9.1 between the nasal organoid derived from the younger adult (28 years old) and that from the older adult (68 years old). The nasal organoid derived from the older adult exhibited a much higher expression the senescence biomarker beta-galactosidase (Figure 3A). We also determined the viral replication in VeroE6/TMPRSS2 cells (a monkey kidney cell line that is most frequently used for viral culture) and A549/TMPRSS2/ACE2 (a human lung cell line derived from a patient with carcinoma that overexpresses the TMPRSS2 and ACE2). There was no statistically significant difference in the virus replication kinetics between EG.5.1 and XBB.1.9.1 in A549/TMPRSS2/ACE2, nasal organoid from the younger adult, and the nasal organoid from the older adult (Figure 3B). On VeroE6/TMPRSS2 cells, the viral load of EG.5.1 was slightly higher than XBB.1.9.1 at 48 hpi (9.675 log10 vs. 9.089 log10). Both EG.5.1 and XBB.1.9.1 achieved highest viral load in the nasal organoid derived from the younger adult and VeroE6/TMPRSS2 cell line. At 24, 48 and 72 hpi, the viral loads in the younger adult nasal organoid were about 1–2 log higher than those in the older adult nasal organoid (Figure S2).

To further compare the fitness of EG.5.1 and XBB.1.9.1, we performed the competition assay in the human nasal organoids. For the nasal organoid derived from the 28-year-old adult, the mean % of EG.5.1 increased from 60% to 74.4% within the first 24 h, but remained below 80% up to 72 hpi (Figure 3C). The viral load was too low in the nasal organoid derived from the older adult for accurate quantification. Hence, we did not observe an improve fitness of EG.5.1 over XBB.1.9.1.

Fusion assay

We previously demonstrated that cell-cell fusion differs between variants.[17] In this study, we compared the fusion activity between EG.5.1 and XBB.1.9.1 in VeroE6/TMPRSS2 cells. There was no observable difference between the cell-cell fusion activity at 24, 48 or 72 hpi (Figure S3).

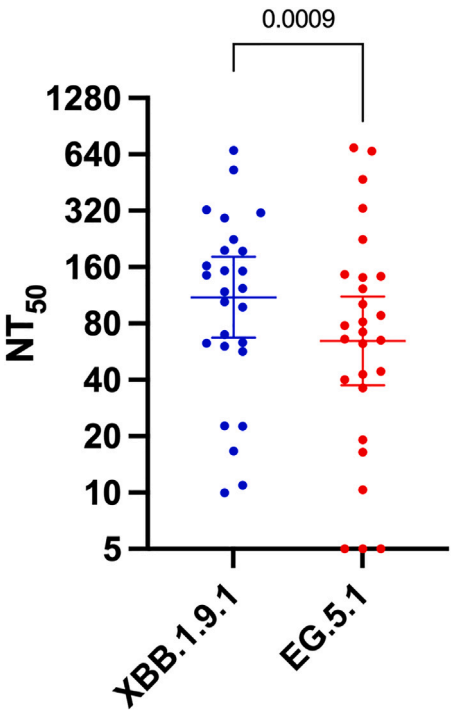

Figure 2. Comparison of live virus neutralizing antibody titers against EG.5.1 and XBB.1.9.1
Serum specimens with undetectable levels of nAb against both EG.5.1 and XBB.1.9.1 were excluded. Dotted horizontal lines represent the lower limit of detection. Data represent the geometric mean titer with 95% confidence interval. Statistical analysis was performed using Wilcoxon matched pairs signed rank test. NT_{50}, 50% neutralization titer.

Cytokine and chemokine response in nasal organoid

Next, we determined whether there is any difference in the ability of EG.5.1 and XBB.1.9.1 in eliciting inflammatory response in the nasal organoid derived from the younger adult. The levels of IL1β, IL6, IP10, IL8, IFNα2 and GM-CSF were not statistically significantly different between EG.5.1 and XBB.1.9.1 (Figure 4). The levels of other cytokines were near the limit of quantification and therefore not compared.

DISCUSSION

The ancestral SARS-CoV-2 strain has undergone significant evolutionary divergences, resulting in the emergence of multiple lineages. Nonetheless, only a limited number of lineages have prevailed.[1] The ability to evade from prior population immunity and increased viral fitness are important attributes leading to the success of a variant.[5,10,16,18] Globally, EG.5 is currently the most prevalent sublineage in October 2023. In Hong Kong, there was a surge of SARS-CoV-2 cases in early summer, with a peak in May 2023 (Figure 1), which was dominated by XBB.1.9, XBB.1.5 and XBB.1.16 at similar proportions. However, the EG.5.1, a descendant of XBB.1.9.1, has replaced other lineages causing a small speak in September/October 2023. In this study, we sought to determine how EG.5.1 outcompeted XBB.1.9.1 and became the dominant lineage. We found that EG.5.1, which contains the spike F456L mutation, was 1.71-fold less susceptible to neutralization by serum collected in August 2023. However, we did not observe any significant increase in fitness of EG.5.1 over XBB.1.9.1 in human bronchial epithelial cell line (A549/TMPRSS2/ACE2) and human nasal organoids. Hence, our findings suggest that the prevalence of EG.5.1 in Hong Kong and globally was more likely attributed to its ability to escape pre-existing population immunity rather than its enhanced viral fitness.

Previous studies compared EG.5.1 with XBB lineages other than those within the XBB.1.9 lineage.[19,20] In our current study, we specifically compared the difference between EG.5.1 and XBB.1.9.1 because both are descendants of the XBB.1.9 lineage. Our comparison will avoid the potential effect of the unique mutations ORF1a A690V and A3143V that are present in the XBB.1.9 lineage. Another unique feature of our study is that we have used authentic viruses instead of pseudoviruses. This is particularly important for the viral fitness and cytokine assays as pseudovirus only contains the spike protein and therefore the effect of infection due to other viral proteins would be missed.

In the spike protein, EG.5.1 differs from XBB.1.9.1 or XBB.1.9.2 in that EG.5.1 carries the F456L mutation. The F456L mutation is likely responsible for the difference in neutralization susceptibility between XBB.1.9.1 and EG.5.1. Using a pseudovirus neutralization assay, Faraone et al. found that XBB.1.5 with F456L is less susceptible to serum neutralization than XBB.1.5 without the F456L mutation.[20] Furthermore, F456L may be associated with increased transmissibility for other lineages. The European Center for Disease Prevention and Control (ECDC) reported that XBB.1.5 carrying the F456L mutation may have increased transmission rates.[13]

In addition to employing commonly used immortalized cell lines for assessing viral fitness, we also incorporated human nasal organoid as a more physiologically relevant model. First, the nasal epithelium represents the initial anatomical site of SARS-CoV-2 infection. Second, the viral load in the nasal epithelium correlates with person-to-person transmissibility.[21] Third, unlike cell lines that comprise of a single cell type, the nasal organoid consists of the ciliated cells, goblet cells and club cells that recapitulates the cell types in the nasal epithelium.

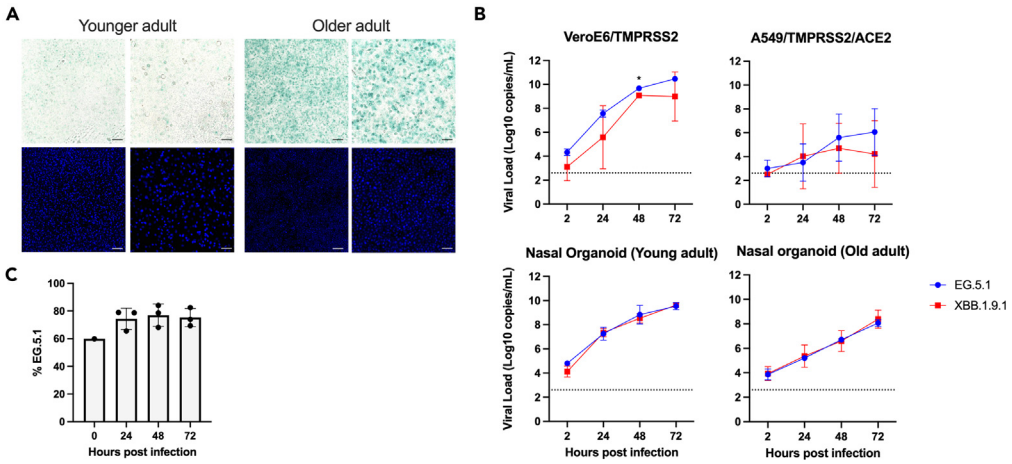

Figure 3. Comparative fitness of EG.5.1 and XBB.1.9.1

(A) Beta-galactosidase staining on differentiated nasal organoid monolayers from a younger adult (28 years old) and an older adult (68 years old). Upper panel: light microscopy; Lower panel: Nuclei were counterstained with DAPI (blue). Scale bar, 100 μm (left), 50 μm (right).

(B) Viral replication in VeroE6/TMPRSS2 cell line, A549/TMPRSS2/ACE2 cell line or nasal organoids derived from the younger adult or the older adult. The viral load was determined using RT-qPCR. Data represent mean, and error bar represents one standard deviation. The viral load at each time point was compared using Student's t test. *, $p < 0.05$.

(C) Competition assay between EG.5.1 and XBB.1.9.1. Human nasal organoid derived from the young adult was infected with EG.5.1 and XBB.1.9.1 at a EG.5.1:XBB.1.9.1 $TCID_{50}$ ratio of 1:1. Next generation sequencing was performed on the cell culture supernatants that were collected at 24, 48 and 72 hpi. The percentage of reads corresponding to the EG.5.1 was determined using the spike amino acid residues 52 and 456. The data at 0 h time point represents the sequencing result of the 1:1 mixture. Data represent mean, and error bar represents one standard deviation.

The host dependent or restriction factors for viral replication are different between human and monkeys (VeroE6), and between the nasal and lung adenocarcinoma cells (A549).

Older adults are more vulnerable to SARS-CoV-2 infection.[3] Hence, risk assessment in this population is especially critical. In the current study, we specifically determined the immune escape of EG.5.1 based on serum of older individuals. Furthermore, we have specifically compared the viral replication in nasal organoids derived from a young and an old adult because there may be age differences in the susceptibility. Indeed, we found that both EG.5.1 and XBB.1.9.1 replicated more slowly in the nasal organoid from the older adult than that derived from the younger adult.

We did not find any significant difference in the cell-cell fusion activity between EG.5.1 and XBB.1.9.1. This is expected as there is no difference in the amino acid sequence between the two virus lineages in the S2 of the spike protein, which is responsible for fusion.

We did not observe with any differences in the cytokine and chemokine response between EG.5.1 and XBB.1.9.1. Our results corroborated with the clinical observation that there is no change in clinical severity for EG.5.1.

The World Health Organization and other public health agencies consider viral genetic and phenotypic characteristics during risk assessment of novel variants. Our data suggest that the risk assessment of novel variants can incorporate data from immune susceptibility testing using a population's serum specimens and viral fitness assessment on human nasal organoid. Since older adults are more vulnerable to SARS-CoV-2 infection, the risk assessment of emerging SARS-CoV-2 variants should include serum specimens and nasal organoid from both younger and older adults.

Limitations of the study

There are several limitations in this study. First, while our results suggest that the nasal epithelium from younger adults are more supportive of SARS-CoV-2 replication, we should interpret the results with caution as our model does not consist of resident or circulating immune cells that limit viral replication. Second, we only tested one strain of each of the lineage. It is possible that viruses within the same lineage may exhibit different immune escape or viral fitness. Third, we only compared nasal organoids derived from one younger adult and one older adult. Comparisons with multiple nasal organoids from young and old adults are required to determine whether this is a general phenomenon.

STAR★METHODS

Detailed methods are provided in the online version of this paper and include the following:

- KEY RESOURCES TABLE
- RESOURCE AVAILABILITY
  - Lead contact
  - Materials availability

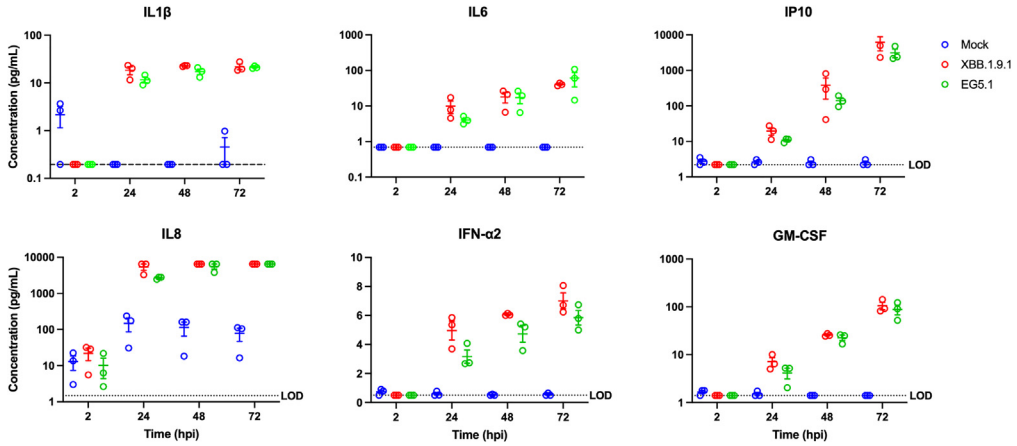

Figure 4. Comparison of cytokine and chemokine response between EG.5.1 and XBB.1.9.1 in human nasal organoid

Human nasal organoid derived from the young adult was infected with EG.5.1 or XBB.1.9.1 at an MOI of 0.1. The levels of cytokines and chemokines were determined in the culture supernatant collected at 2, 24, 48 and 72 hpi. Dotted lines represent the limit of detection. Data represent mean, and the error bars indicate one standard deviation.

SUPPLEMENTAL INFORMATION

Supplemental information can be found online at https://doi.org/10.1016/j.isci.2024.109706.

ACKNOWLEDGMENTS

We gratefully acknowledge the authors originating and submitting laboratories of the SARS-CoV-2 genetic sequences and metadata made available through GISAID. This study was partly supported by the Health and Medical Research Fund, the Food and Health Bureau, the Government of the Hong Kong Special Administrative Region (HKSAR) (COVID1903010 [Project 1] and 22210852); the Theme-Based Research Scheme of the Research Grants Council, HKSAR (Ref no. T11-709/21-N); the Partnership Programme of Enhancing Laboratory Surveillance and Investigation of Emerging Infectious Diseases and Antimicrobial Resistance for the Department of Health, HKSAR; Health@InnoHK, the Innovation and Technology Commission of HKSAR; the Emerging Collaborative Project of Guangzhou Laboratory (EKPG22-01], and National Key R&D Program of China (projects 2021YFC0866100 and 2023YFC3041600). We acknowledge funding received from private donors including Richard Yu and Carol Yu, Shaw Foundation Hong Kong, Michael Seak-Kan Tong, May Tam Mak Mei Yin, Lee Wan Keung Charity Foundation Limited, Providence Foundation Limited (in memory of the late Lui Hac-Minh), Hong Kong Sanatorium & Hospital, Respiratory Viral Research Foundation Limited, Hui Ming, Hui Hoy and Chow Sin Lan Charity Fund Limited, Chan Yin Chuen Memorial Charitable Foundation, Marina Man-Wai Lee, the Hong Kong Hainan Commercial Association South China Microbiology Research Fund, the Jessie & George Ho Charitable Foundation, Kai Chong Tong, Tse Kam Ming Laurence, Foo Oi Foundation Limited, Betty Hing-Chu Lee, and Ping Cham So. The funding sources had no role in the study design, data collection, analysis, interpretation, or writing of the report.

AUTHOR CONTRIBUTIONS

Conceptualization, X.Z., S.J.A.L., J.D.I., C.H.Y.F., and K.K.W.T.; Methodology, X.J., S.J.A.L., J.D.I., C.H.Y.F., A.W.H.C., W.M.C., L.L.C., S.Y., H.Z., and J.Z.; Investigation, X.J., S.J.A.L., J.D.I., C.H.Y.F., A.W.H.C., W.M.C., Y.S.Y.L., H.W.T., B.P.C.C., L.L.C., X.M., and H.Z.; Writing – Original Draft, X.J. and K.K.W.T.; Writing – Review & Editing, X.J., S.J.A.L., J.D.I., C.H.Y.F., A.W.H.C., W.M.C., Y.S.Y.L., H.W.T., B.P.C.C., L.L.C., X.M., S.Y., H.Z., V.C.C.C., J.K.Y.Y., K.Y.Y., J.Z., and K.K.W.T.; Supervision, K.K.W.; Funding Acquisition, K.Y.Y. and K.K.W.T.

DECLARATION OF INTERESTS

All authors declare no conflict of interest.

Received: December 1, 2023
Revised: February 23, 2024
Accepted: April 6, 2024
Published: April 9, 2024

REFERENCES

1. Markov, P.V., Ghafari, M., Beer, M., Lythgoe, K., Simmonds, P., Stilianakis, N.I., and Katzourakis, A. (2023). The evolution of SARS-CoV-2. Nat. Rev. Microbiol. *21*, 361–379. https://doi.org/10.1038/s41579-023-00878-2.
2. Viana, R., Moyo, S., Amoako, D.G., Tegally, H., Scheepers, C., Althaus, C.L., Anyaneji, U.J., Bester, P.A., Boni, M.F., Chand, M., et al. (2022). Rapid epidemic expansion of the SARS-CoV-2 Omicron variant in southern Africa. Nature *603*, 679–686. https://doi.org/10.1038/s41586-022-04411-y.
3. Chen, L.L., Abdullah, S.M.U., Chan, W.M., Chan, B.P.C., Ip, J.D., Chu, A.W.H., Lu, L., Zhang, X., Zhao, Y., Chuang, V.W.M., et al. (2022). Contribution of low population immunity to the severe Omicron BA.2 outbreak in Hong Kong. Nat. Commun. *13*, 3618. https://doi.org/10.1038/s41467-022-31395-0.
4. Chen, L.L., Chua, G.T., Lu, L., Chan, B.P.C., Wong, J.S.C., Chow, C.C.K., Yu, T.C., Leung, A.S.Y., Lam, S.Y., Wong, T.W., et al. (2022). Omicron variant susceptibility to neutralizing antibodies induced in children by natural SARS-CoV-2 infection or COVID-19 vaccine. Emerg. Microbes Infect. *11*, 543–547. https://doi.org/10.1080/22221751.2022.2035195.
5. Lu, L., Mok, B.W.Y., Chen, L.L., Chan, J.M.C., Tsang, O.T.Y., Lam, B.H.S., Chuang, V.W.M., Chu, A.W.H., Chan, W.M., Ip, J.D., et al. (2022). Neutralization of Severe Acute Respiratory Syndrome Coronavirus 2 Omicron Variant by Sera From BNT162b2 or CoronaVac Vaccine Recipients. Clin. Infect. Dis. *75*, e822–e826. https://doi.org/10.1093/cid/ciab1041.
6. Yuan, S., Ye, Z.W., Liang, R., Tang, K., Zhang, A.J., Lu, G., Ong, C.P., Man Poon, V.K., Chan, C.C.S., Mok, B.W.Y., et al. (2022). Pathogenicity, transmissibility, and fitness of SARS-CoV-2 Omicron in Syrian hamsters. Science *377*, 428–433. https://doi.org/10.1126/science.abn8939.
7. Karim, S.S.A., and Karim, Q.A. (2021). Omicron SARS-CoV-2 variant: a new chapter in the COVID-19 pandemic. Lancet *398*, 2126–2128. https://doi.org/10.1016/S0140-6736(21)02758-6.
8. Cheng, V.C.C., Ip, J.D., Chu, A.W.H., Tam, A.R., Chan, W.M., Abdullah, S.M.U., Chan, B.P.C., Wong, S.C., Kwan, M.Y.W., Chua, G.T., et al. (2022). Rapid Spread of Severe Acute Respiratory Syndrome Coronavirus 2 (SARS-CoV-2) Omicron Subvariant BA.2 in a Single-Source Community Outbreak. Clin. Infect. Dis. *75*, e44–e49. https://doi.org/10.1093/cid/ciac203.
9. Roemer, C., Sheward, D.J., Hisner, R., Gueli, F., Sakaguchi, H., Frohberg, N., Schoenmakers, J., Sato, K., O'Toole, Á., Rambaut, A., et al. (2023). SARS-CoV-2 evolution in the Omicron era. Nat. Microbiol. *8*, 1952–1959. https://doi.org/10.1038/s41564-023-01504-w.
10. Zhang, X., Chen, L.L., Ip, J.D., Chan, W.M., Hung, I.F.N., Yuen, K.Y., Li, X., and To, K.K.W. (2023). Omicron sublineage recombinant XBB evades neutralising antibodies in recipients of BNT162b2 or CoronaVac vaccines. Lancet. Microbe *4*, e131. https://doi.org/10.1016/S2666-5247(22)00335-4.
11. World Health Organization (2023). Tracking SARS-CoV-2 variants. https://www.who.int/activities/tracking-SARS-CoV-2-variants.
12. World Health Organization (2023). EG.5 Updated Risk Evaluation, 21 September 2023. https://www.who.int/docs/default-source/coronaviruse/eg5-risk-evaluation.pdf?sfvrsn=6e9690e0_4.
13. European Centre for Disease and Prevention (2023). ECDC classifies XBB.1.5-like lineages with the amino acid change F456L as variants of interest following an increase in SARS-CoV-2 transmission in EU/EEA countries and abroad. https://www.ecdc.europa.eu/en/news-events/ecdc-classifies-xbb15-lineages-amino-acid-change-f456l-variants-interest-following.
14. The World Health Organization (2023). COVID-19 Epidemiological Update - 27 October 2023. https://www.who.int/publications/m/item/covid-19-epidemiological-update—27-october-2023.
15. Chiu, M.C., Li, C., Liu, X., Song, W., Wan, Z., Yu, Y., Huang, J., Xiao, D., Chu, H., Cai, J.P., et al. (2022). Human Nasal Organoids Model SARS-CoV-2 Upper Respiratory Infection and Recapitulate the Differential Infectivity of Emerging Variants. mBio *13*, e0194422. https://doi.org/10.1128/mbio.01944-22.
16. Li, C., Huang, J., Yu, Y., Wan, Z., Chiu, M.C., Liu, X., Zhang, S., Cai, J.P., Chu, H., Li, G., et al. (2023). Human airway and nasal organoids reveal escalating replicative fitness of SARS-CoV-2 emerging variants. Proc. Natl. Acad. Sci. USA *120*, e2300376120. https://doi.org/10.1073/pnas.2300376120.
17. Zhao, H., Lu, L., Peng, Z., Chen, L.L., Meng, X., Zhang, C., Ip, J.D., Chan, W.M., Chu, A.W.H., Chan, K.H., et al. (2022). SARS-CoV-2 Omicron variant shows less efficient replication and fusion activity when compared with Delta variant in TMPRSS2-expressed cells. Emerg. Microbes Infect. *11*, 277–283. https://doi.org/10.1080/22221751.2021.2023329.
18. Meijers, M., Ruchnewitz, D., Eberhardt, J., Łuksza, M., and Lässig, M. (2023). Population immunity predicts evolutionary trajectories of SARS-CoV-2. Cell *186*, 5151–5164.e13. https://doi.org/10.1016/j.cell.2023.09.022.
19. Wang, Q., Guo, Y., Liu, L., Schwanz, L.T., Li, Z., Nair, M.S., Ho, J., Zhang, R.M., Iketani, S., Yu, J., et al. (2023). Antigenicity and receptor affinity of SARS-CoV-2 BA.2.86 spike. Nature *624*, 639–644. https://doi.org/10.1038/s41586-023-06750-w.
20. Faraone, J.N., Qu, P., Goodarzi, N., Zheng, Y.M., Carlin, C., Saif, L.J., Oltz, E.M., Xu, K., Jones, D., Gumina, R.J., and Liu, S.L. (2023). Immune evasion and membrane fusion of SARS-CoV-2 XBB subvariants EG.5.1 and XBB.2.3. Emerg. Microbes Infect. *12*, 2270069. https://doi.org/10.1080/22221751.2023.2270069.
21. Trunfio, M., Richiardi, L., Alladio, F., Staffilano, E., Longo, B., Venuti, F., Ghisetti, V., Burdino, E., Bonora, S., Vineis, P., et al. (2022). Determinants of SARS-CoV-2 Contagiousness in Household Contacts of Symptomatic Adult Index Cases. Front. Microbiol. *13*, 829393. https://doi.org/10.3389/fmicb.2022.829393.
22. Shu, Y., and McCauley, J. (2017). GISAID: Global initiative on sharing all influenza data - from vision to reality. Euro Surveill. *22*, 30494. https://doi.org/10.2807/1560-7917.ES.2017.22.13.30494.
23. Van Rosuum, G., and Drake Jr, F.L. (2023). Python v3.9.12. https://www.python.org/.
24. McKinney, W. (2010). Data Structures for Statistical Computing in Python. In Proceedings of the 9th Python in Science Conference, 445Proceedings of the 9th Python in Science Conference, pp. 51–56.

STAR★METHODS

KEY RESOURCES TABLE

REAGENT or RESOURCE	SOURCE	IDENTIFIER
Bacterial and virus strains		
hCoV-19/Hong Kong/HKU-231103-001/2023	In house	N/A
hCoV-19/Hong Kong/HKU-230414-002/2023	In house	N/A
Chemicals, peptides, and recombinant proteins		
10X TrypLE Select	Gibco™; New York, USA	Cat# A1217701
Matrigel	Corning®, Corning, NY, USA	Cat# 356231
PneumaCult™-ALI Medium	Vancouver, BC, Canada,	Cat# 05001
Fetal bovine serum	Gibco™; New York, USA	Cat# 16140071
Dulbecco's Modified Eagle Medium (DMEM)	Gibco™; New York, USA	Cat# 2523099
Penicillin/streptomycin	Gibco™; New York, USA	Cat# 15140122
phosphate-buffered saline (PBS)	Gibco™; New York, USA	Cat# 2430052
Low-melting point agarose	InvivoGen	Cat# 16520100
Crystal violet	Sigma-Aldrich®, Saint Louis, MO, USA	Cat# 548-62-9
Polyethylenimine MAX (PEI MAX)	Polysciences	Cat# 24756-1
4′,6-diamidino-2-phenylindole	Vector Laboratories, Burlingame, CA, USA	Cat# H-1200-10
Critical commercial assays		
β-Galactosidase Staining Kit	Danvers, MA, USA	Cat# 9860
LEGENDplex™	BioLegend, San Diego	Cat# 740390
RNeasy Mini Kit	QIAGEN	Cat# 74104
Deposited data		
Full genome sequence of SARS-CoV-2 EG.5.1 virus	GISAID	EPL_ISL_18461518
Full genome sequence of SARS-CoV-2 XBB.1.9.1 virus	GISAID	EPI_ISL_17468452
Experimental models: Cell lines		
VeroE6/TMPRSS2	JCRB	Cat# JCRB1819 RRID: CVCL_YQ49
A549/TMPRSS2/ACE2	InvivoGen	a549-hace2tpsa RRID: CVCL_A5KB
Oligonucleotides		
Rdrp/Hel Forward primer CGCATACAGTCTTRCAGGCT	Integrated DNA Technologies	N/A
Rdrp/Hel Reverse primer GTGTGATGTTGAWATGACATGGTC	Integrated DNA Technologies	N/A
Rdrp/Hel Probe FAM-TTAAGATGTGGTGCTTGCATACGTAGAC-lABkFQ	Integrated DNA Technologies	N/A
Software and algorithms		
GraphPad Prism	GraphPad	https://www.graphpad.com
Anaconda Software Distribution	Anaconda	https://www.anaconda.com/downloads

RESOURCE AVAILABILITY

Lead contact

Further information and requests for resources and reagents should be directed to and will be fulfilled by the lead contact, Kelvin Kai-Wang To (kelvinto@hku.hk).

Materials availability

This study did not generate new unique reagents.

Data and code availability

The genome sequences of viral strains used in this study are deposited to GISAID (Accession number: EPL_ISL_18461518 and EPI_ISL_17468452). All data reported in this paper will be shared by the lead contact upon request. This paper does not report original code. Any additional information required to reanalyze the data reported in this paper is available from the lead contact upon request.

EXPERIMENTAL MODEL AND STUDY PARTICIPANT DETAILS

Ethical approval

This study has been approved by the Institutional Review Board of the University of Hong Kong/Hospital Authority of Hong Kong West Cluster (HKU/HA HKW IRB) (Reference number UW 22–328 and UW 23–376).

Global prevalence of XBB.1.9.1 and EG.5 sublineages

We downloaded the metadata of SARS-CoV-2 sequences from GISAID on 6th November 2023.[22] A SARS-CoV-2 sequence was included if it had been marked as complete in the metadata file, and was directly obtained from a human clinical specimen without *in vitro* passage. A sequence was excluded if collection date information was not complete. All processing was performed on Python v3.9.12[23] (pandas v1.4.2,[24] json v2.0.9) running on Anaconda Software Distribution v 4.11.0.

Cell lines

TMPRSS2-expressing VeroE6 (VeroE6/TMPRSS2) cell line was obtained from the Japanese Collection of Research Bioresources (JCRB) Cell Bank (JCRB Cat#JCRB1819). TMPRSS2 and ACE2 over-expressing A549 cells (A549/TMPRSS2/ACE2) were obtained from InvivoGen (Catalog code: a549-hace2tpsa).

Virus strains

The SARS-CoV-2 EG.5.1 (GISAID accession number: EPL_ISL_18461518) and XBB.1.9.1 strains (GISAID accession number EPI_ISL_17468452) were isolated from respiratory specimens of COVID-19 patients in Hong Kong. The virus isolates were cultured using VeroE6/TMPRSS2 cells and was performed in a biosafety level 3 facility as we described previously.[10]

METHOD DETAILS

Live virus neutralization test

Serum samples collected from 33 adults aged over 70 years old in Hong Kong were heat-inactivated at 56°C for 30 min and were serially diluted in 2-folds with MEM containing 1% fetal bovine serum (FBS). Duplicates of each diluted serum were mixed with a SARS-CoV-2 virus isolate to reach a final concentration of 100 $TCID_{50}$ and were incubated at 37°C for 1 h. After incubation, 100 μL of the serum-virus mixture was then added to VeroE6/TMPRSS2 cells that were seeded in 96-well plates 24 h before infection. The cells were incubated with the mixture at 37°C. After incubation for 3 days, cytopathic effect (CPE) was visually scored for each well by two independent observers in a blinded manner. The 50% neutralisation titer (NT_{50}) was determined by using log (inhibitor) vs. normalized response-variable slope in GraphPad PRISM version 9.4.0. For statistical analysis, a value of 5 was assigned if the live virus neutralising antibody titer is < 10.

Human nasal organoids

Nasal cells collected from the nasal mid-turbinate were washed and digested into single cells with 10X TrypLE Select (Gibco; New York, USA; Cat#A1217701). Resultant cells were embedded in 70% Matrigel (Corning, Corning, NY, USA, Cat#356231) and supplemented with expansion medium in a 24-well suspension culture plate (Thermo Scientific, Rochester, NY, USA, Cat#144530). Details of the expansion medium is shown in Table S2. The organoids were passaged once they reach 70–80% confluency (i.e., every 7–14 days).

To develop differentiated nasal organoid monolayers (dNsO-mono), we first digested undifferentiated 3D nasal organoids into single cells with 10X TrypLE Select for 3–5 min at 37°C and seeded the cells onto Transwell inserts (Corning, NY, USA; Cat#3470). The cells were cultured in expansion medium for 3 to 4 days to reach 90% confluency. Differentiation was then initiated by switching to differentiation medium (PneumaCult-ALI Medium [STEMCELL Technologies]; Vancouver, BC, Canada, Cat# 05001) supplemented with 10 mM N-[N-(3,5-difluorophenacetyl)-*l*-alanyl]-S-phenylglycine *t*-butyl ester (DAPT) and incubated for another 10 to 12 days. The medium was supplied to both the upper and lower compartments and was replenished every other day.

β-galactosidase staining

β-galactosidase staining was performed using Cell Signaling Technology's Senescence β-Galactosidase Staining Kit (Danvers, MA, USA Cat#9860). dNsO-mono fixed overnight at 4°C were stained according to the manufacturer's protocol. Images were acquired using the Olympus BX53F microscope.

Viral replication kinetics in VeroE6/TMPRSS2 cell line, A549/TMPRSS2/ACE2 cell line

VeroE6/TMPRSS2 or A549/TMPRSS2/ACE2 cells were seeded onto 96-well tissue culture plates with Dulbecco's Modified Eagle Medium (DMEM) supplemented with 10% FBS, 100 U/mL of penicillin, and 100 μg/mL of streptomycin. The culture plates were incubated at 37°C and 5% CO_2 for 48 h prior to the experiment. After removing the culture medium and washing cells by phosphate-buffered saline (PBS), 0.01 multiplicity of infection (MOI) of EG.5.1 or XBB.1.9.1 were inoculated to cells for infection at 37°C and 5% CO_2 for 2 h. Cell culture supernatant was collected at 2, 24, 48, and 72 h post infection (hpi). Viral RNA was extracted for RT-qPCR assay to determine the viral load. Cell lysates were collected at 72 hpi.

Viral replication kinetics in human nasal organoids

Human nasal organoids were infected with EG.5.1 or XBB.1.9.1 at 0.1 MOI. The infected nasal organoids were incubated at 37°C in a 5% CO_2 incubator. After 2 h of viral adsorption, the medium was removed. Organoids were washed twice with basal medium and cultured with basal medium at 37°C and 5% CO_2 incubator. The supernatant was collected at 2, 24, 48 and 72 hpi. At each of the time points, the viral load in the culture supernatant was determined by RT-qPCR, and the viral titer was determined by plaque assay.

Determination of viral load with RT-qPCR

Viral RNA was extracted with RNA mini kit (Qiagen) for viral load assays. The viral load was determined using reverse transcription quantitative polymerase chain reaction (RT-qPCR) targeting the RdRp gene.

Plaque assay

The VeroE6/TMPRSS2 cells were seeded one day before infection at 1.5×10^6 cells/mL. On the day of infection, cells were infected with 10-fold serial dilutions of culture supernatant and incubated at 37°C, 5% CO_2 incubator for 1 h. At the end of the incubation, the culture supernatant was removed and replaced with 2× MEM medium and 2% low-melting point agarose mixture. At 3 days post-infection, the cells were fixed with 4% formaldehyde in PBS overnight and the cells were stained with 0.5% crystal violet solution (80% of PBS and 20% methanol). The cells were then washed to reveal the plaques. The result was expressed as plaque-forming units (PFU)/mL.

Competition assay in human nasal organoids

Human nasal organoids were infected with 0.1 MOI of EG.5.1 and XBB.1.9.1 at a ratio of 1:1 based on the $TCID_{50}$ as determined in VeroE6/TMPRSS2 cells. Culture supernatant was collected at 24, 48 and 72 hpi for whole viral genome sequencing. Biological triplicate was performed.

Whole-genome sequencing was performed using Illumina sequencing. The percentage of reads corresponding to the EG.5.1 and XBB.1.9.1 at the spike amino acid residues 52 (EG.5.1: H; XBB.1.9.1: Q) and 456 (EG.5.1: L; XBB.1.9.1: F) was used for the determination of competition results.

Cytokine and chemokine assay

The levels of cytokines and chemokines in the culture supernatant were measured using the multiplex panel (LEGENDplex) (BioLegend, San Diego, Cat no. 740390). The cytokine and chemokines included IL1β, IL6, TNFα, IP10, IFNα2, IFNβ, IFNλ1, IFNλ2/3, IFNγ, IL8, IL12p70, GM-CSF and IL10.

Fusion assay

Green fluorescent protein (GFP) plasmid was packaged by Polyethylenimine MAX (PEI MAX) (Polysciences, Cat no: 24756-1) and transfected into VeroE6/TMPRSS2 cells in 24-well plates. At 8 h post transfection, 0.0001 MOI of EG.5.1 or XBB.1.9.1 was added to GFP-transfected cells. At 24, 48, and 72 hpi, cell images were taken with fluorescent microscope. GFP-transfected cells without viral infection represent the negative control for virus-induced cell-cell fusion.

QUANTIFICATION AND STATISTICAL ANALYSIS

Statistical analysis was performed using GraphPad Prism 10.2.0. The viral loads at each time point between XBB.1.9.1 and EG.5.1, and between EG.5.1 and BA.5.2, were compared using Student's t test. A p value of <0.05 was considered as statistically significant.